Pumping new life into preclinical pharmacokinetics: exploring the pharmacokinetic application of ex vivo organ perfusion

Stevens, L.J.

PART III

Unraveling pharmacokinetics through multi-organ perfusion

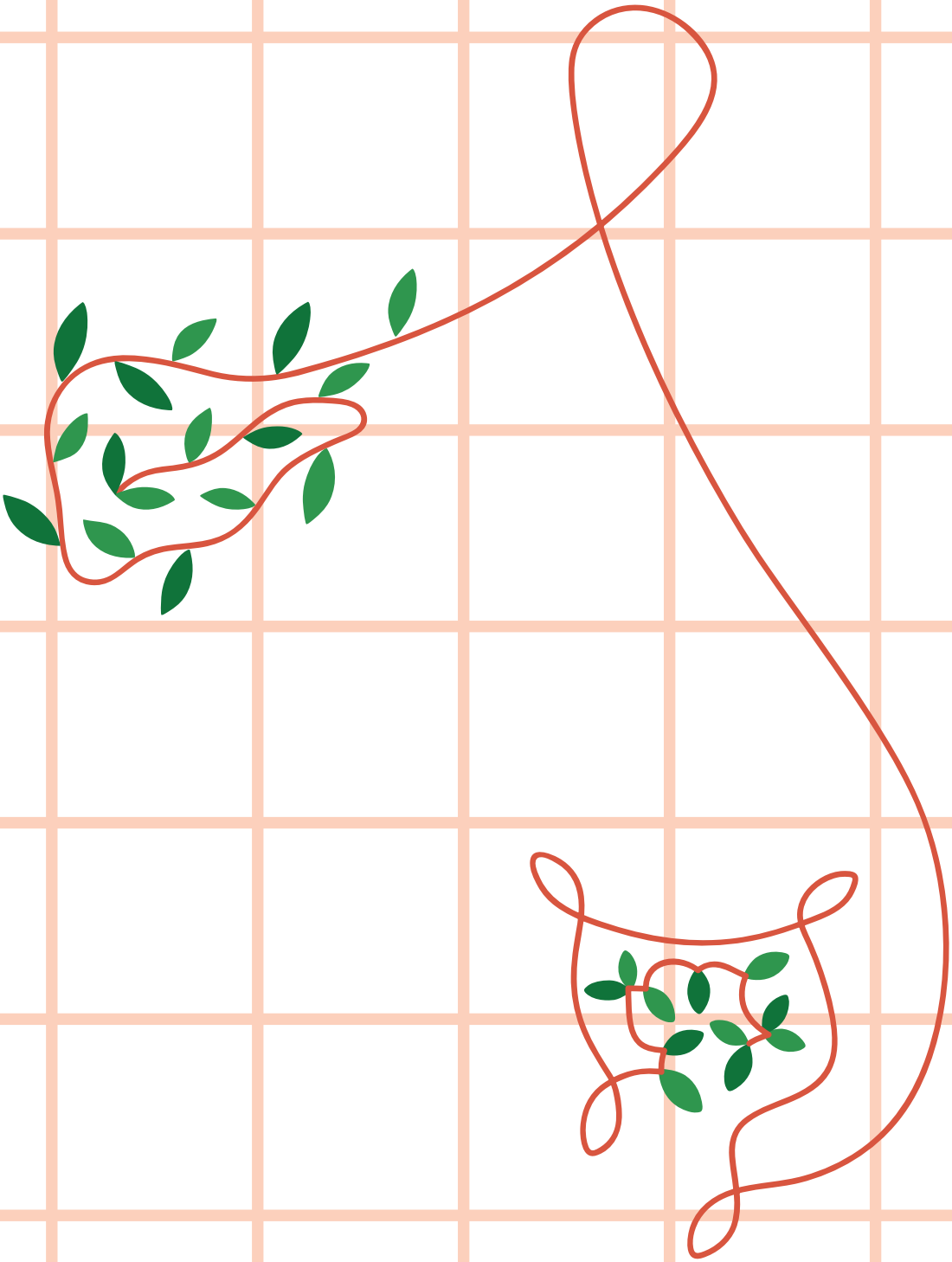

CHAPTER 06

Ex vivo Gut-Hepato-Biliary organ perfusion model to characterize oral absorption, gut-wall metabolism, pre-systemic hepatic metabolism and biliary excretion; application to midazolam

L.J. Stevens, E. van de Steeg, J.B. Doppenberg, I.P.J. Alwayn, C.A.J. Knibbe, J. Dubbeld

European Journal of Pharmaceutical sciences, 2024

Abstract

To date, characterization of the first-pass effect of orally administered drugs consisting of local intestinal absorption and metabolism, portal vein transport and hepatobiliary processes remains challenging. Aim of this study was to explore the applicability of a porcine ex-vivo perfusion model to study oral absorption, gut-hepatobiliary metabolism and biliary excretion of midazolam.

Slaughterhouse procured porcine *en bloc* organs (n=4), were perfused via the aorta and portal vein. After 120min of perfusion, midazolam, atenolol, antipyrine and FD4 were dosed via the duodenum and samples were taken from the systemic- and portal vein perfusate, intestinal faecal effluent and bile to determine drug and metabolite concentrations.

Stable arterial and portal vein flow was obtained and viability of the perfused organs was confirmed. After intraduodenal administration, midazolam was rapidly detected in the portal vein together with 1-OH midazolam ($E_{G\text{-}pv}$ of 0.16±0.1) resulting from gut wall metabolism through oxidation. In the intestinal faecal effluent, 1-OH midazolam and 1-OH midazolam glucuronide ($E_{G\text{-}intestine}$ 0.051±0.03) was observed resulting from local gut glucuronidation. Biliary elimination of midazolam (0.04±0.01%) and its glucuronide (0.01±0.01%) only minimally contributed to the enterohepatic circulation. More extensive hepatic metabolism (F_H 0.35±0.07) over intestinal metabolism (F_G 0.78±0.11) was shown, resulting in oral bioavailability of 0.27±0.05.

Ex vivo perfusion demonstrated to be a novel approach to characterize pre-systemic extraction of midazolam by measuring intestinal as well as hepatic extraction. The model can generate valuable insights into the absorption and metabolism of new drugs.

Introduction

In order to determine the oral bioavailability of a drug, characterization of gut-wall, liver and biliary processes is of great importance[1]. Insight into the extent of intestinal absorption and metabolism, portal venous blood concentrations and hepatic metabolism and biliary excretion is crucial in the early stages of drug development to understand the pharmacokinetics (PK) and select compounds that achieve a desirable systemic exposure. This is especially the case for compounds prone to CYP3A metabolism which reduce the oral bioavailability due to first-pass metabolism in both the gut wall and liver. Oral bioavailability, determined by the fraction absorbed (F_a), fraction escaping gut-wall elimination (F_G) and fraction escaping hepatic elimination (F_H) show the importance of the intestine and liver in this process[2].

However, the assessment of F_a, F_G and F_H is extremely challenging and rarely performed due to ethical and technical reasons[3,4]. Therefore, preclinical evaluation is needed to assess the oral absorption and concentrations of drug and metabolite in the systemic circulation. The possibility to study F_G and F_H in a preclinical *in vitro* model is also limited as it remains difficult to recapitulate complete organ function behaviour within a single model. Such a single model could provide highly relevant information in early drug development for several fields of research, for example, in physiologically based pharmacokinetic (PBPK) modelling prediction. This is especially crucial as precise predictions can effectively reduce attrition and failure rates within the drug development process, while also aiding in the determination of initial starting dosages of compounds[5]. Recent advancements in organ perfusion techniques have created new opportunities for studying physiological processes in an *ex vivo* setting. Normothermic machine perfusion (NMP) has been demonstrated in numerous studies to maintain *ex vivo* liver, kidney, pancreas and even intestinal function for several hours[6-9]. In the field of pharmacology, NMP has proven to be advantageous for determining the hepatic and biliary clearance as well as renal clearance[10-13]. The intact vasculature and presence of the elimination routes of these whole-organ models offers greater potential of studying absorption, distribution, metabolism and elimination (ADME) process compared to cellular preclinical systems[14]. While the majority of studies focus on perfusion with a single organ, a few studies have investigated the possibility of a multi-organ perfusion model to study physiological processes[15-18]. These studies, combining liver and kidneys in one circuit, show that combination of organs is

beneficial for the biochemical environment and as well can reduce the impact of warm ischemia and reperfusion injury[16,19]. Together, the option to perfuse multiple organs allows in-depth analysis of ADME processes like gut wall metabolism, portal vein concentrations, hepatic uptake and biliary excretion. Simultaneously, it maintains a favourable biochemical environment through the inclusion of homeostatic organs.

The aim of the study was to explore the applicability of a porcine *ex vivo* perfusion model to characterize oral absorption, gut wall metabolism, first pass hepatic metabolism and biliary excretion by pre-systemic measurements of midazolam and metabolite concentrations in portal vein, intestinal faecal effluent and systemic and bile measurement.

Materials and methods

Chemicals

Heparin, sodium taurocholate, insulin, dexamethasone, atenolol, antipyrine and FD4 were purchased from Sigma-Aldrich, Zwijndrecht, the Netherlands. Epoprostenol was purchased from R&D systems (Minneapolis, USA). Calcium gluconate 10% was obtained from Pharmamarket (Hove, Belgium). Aminoplasmal 10E was obtained from (B Braun Melsungen AG, Melsungen, Germany). Midazolam was obtained from Spruyt Hillen (Ijsselstein, the Netherlands).

Organ procurement

En bloc organs were obtained from a local slaughterhouse, in compliance with the guidelines of the Dutch food safety authority. Pigs (*Netherlands Landrace*, approximately 6 months of age with body weight between 100 and 120 kg) were anesthetized by a standardized procedure of electrocution followed by exsanguination (termination). Three liters of blood was collected during exsanguination in a container supplemented with 25000 IU of heparin. Per industry guidelines, carcasses were cleaned in a pig washing & whipping machine using 70°C water for approximately 3-5 minutes and dehaired through scalding. Slaughter offal was dissected from the carcasses, keeping all organs and vascular structures intact.

Porcine *en bloc* organ preservation and model development

After receiving the organ package, the heart, lungs and esophagus were dissected. Thereafter the abdominal aorta was proximally cannulated (25 Fr). In order to create a closed abdominal compartment for arterial perfusion, the abdominal aorta was ligated distal from the renal arteries. The lumbar arteries were separately ligated. A cold flush was initiated within ~15 min after termination (warm ischemic time), using Histidine-Tryptophan-Ketoglutarate (HTK) solution (Plegistore, Warszawa in Poland) by applying a pressure of 80 mmHg (pressure bag Endomed, Uden, the Netherlands). During the flush, the entire colon was dissected from the organ package. After approximately 7L of HTK solution, an additional portal flush was performed. The portal vein was partially dissected and cannulated at both ends (Supplemental Figure S6.1) resulting in 1) portal vein – intestinal side cannulation (25 Fr) (efferent), and 2) a portal vein – liver side (afferent), (25 Fr). Additional flush at the portal vein – liver side was applied with 2L of HTK. Thereafter, the organs were transported on static cold storage. At the laboratory, the stomach was removed and the small intestine was shortened to approximately 2 meters preserving the duodenum and the proximal part of the jejunum (~1.5 meter). A cannula was placed in the orifice of the duodenum to allow for administration of (dissolved) compounds. A clamp was placed on the cannula before and after administration of compound(s) in order to prevent backflow. To make intestinal outflow possible at the jejunal side, a second cannula was inserted. Thereafter the common bile duct was cannulated to the liver side, while the *cystic duct,* derived from the gall bladder, was ligated to restrict bile flow to the gall bladder. Lastly, the ureters were cannulated which was the final step before initiation of normothermic perfusion.

Normothermic machine perfusion

The porcine organs (n=4) were perfused using the Liver Assist™ device (XVIVO, Groningen, the Netherlands) (Figure 6.1A-B). The reservoir included in the disposable set was too small to fit the organs, therefore a custom made organ reservoir was made. The newly developed reservoir consisted of a box (60x40x20 cm box) with a built in drain connecting the box with the Liver Assist reservoir. An mesh basket (60x40x15 cm) was suspended in the box. The organs were placed in the mesh basket, enabling the venous outflow of the organs flowing in the box and subsequently to the Liver Assist reservoir via the drain. The system was filled with 3 liter perfusion fluid containing autologous

red blood cells and plasma (ratio 1:1), supplemented with 10 mL (10%) mannitol and 18 mg dexamethasone, 75µg epoprostenol and 10 mL 10% calcium gluconate. Insulin, taurocholate, heparin, epoprostenol and aminoplasmal 10E were provided as continuous infusion at a rate of 10 U/h, 1041 U/h, 10 mL/h (2% w/v), 8 µg/h and 10 mL/hr respectively to keep the liver metabolically active[13]. Gas delivery to the Liver Assist™ device consisted of 40% oxygen at 1.5 L/min and the temperature was set at 39°C. An arterial pressure was set at 60-80 mmHg. Due to reduction in the intestinal length and thereby reduction in the vascular bed, the portal vein flow could result in an insufficient flow. Therefore, portal perfusion was applied via the portal vein-liver side (Supplemental Figure S6.1), with a pressure between 8-11 mmHg. The aorta and portal vein received perfusate from the reservoir, venous outflow of the organs was open and flowed back to the reservoir (Figure 6.1B). Continuous recirculation of the perfusate was applied. During normothermic perfusion, absorption of fluid into the intestine was observed. To retain a sufficient perfusate level, red blood cells and plasma of a blood type-matched pig was used when a decrease in hematocrit was observed (<20% hematocrit), otherwise ringers lactate was used to replenish the perfusate level. The *en bloc* organs were perfused for a total time of 420 minutes.

Drug administration during normothermic perfusion

20 mg midazolam, 25 mg atenolol, 50 mg antipyrine and 1 mL of 10 mM FITC-Dextran 4000 (FD4) were dissolved in Williams E medium (50 mL) and dosed via the cannula in the duodenum. Exact luminal concentration of the compounds is not known since luminal fluid was already present in the intestine resulting in further dilution of the compounds. T=0 min was defined as time of starting the bolus into the duodenum. Subsequently, intestinal faecal effluent, portal vein perfusate, systemic perfusate and bile samples were taken for the following 240 min at time points t=0, 15, 30, 45, 60, 90, 120, 150, 180, 210 and 240 min after dosing. Samples were centrifuged directly after collection and immediately stored at ≤-70°C until further processing. Drug concentrations of midazolam, 1-OH midazolam, 1-OH midazolam glucuronide, atenolol and antipyrine in the portal vein perfusate, systemic perfusate, intestinal faecal effluent, bile and tissue were determined by LC-MS/MS and UPLC analysis as described below.

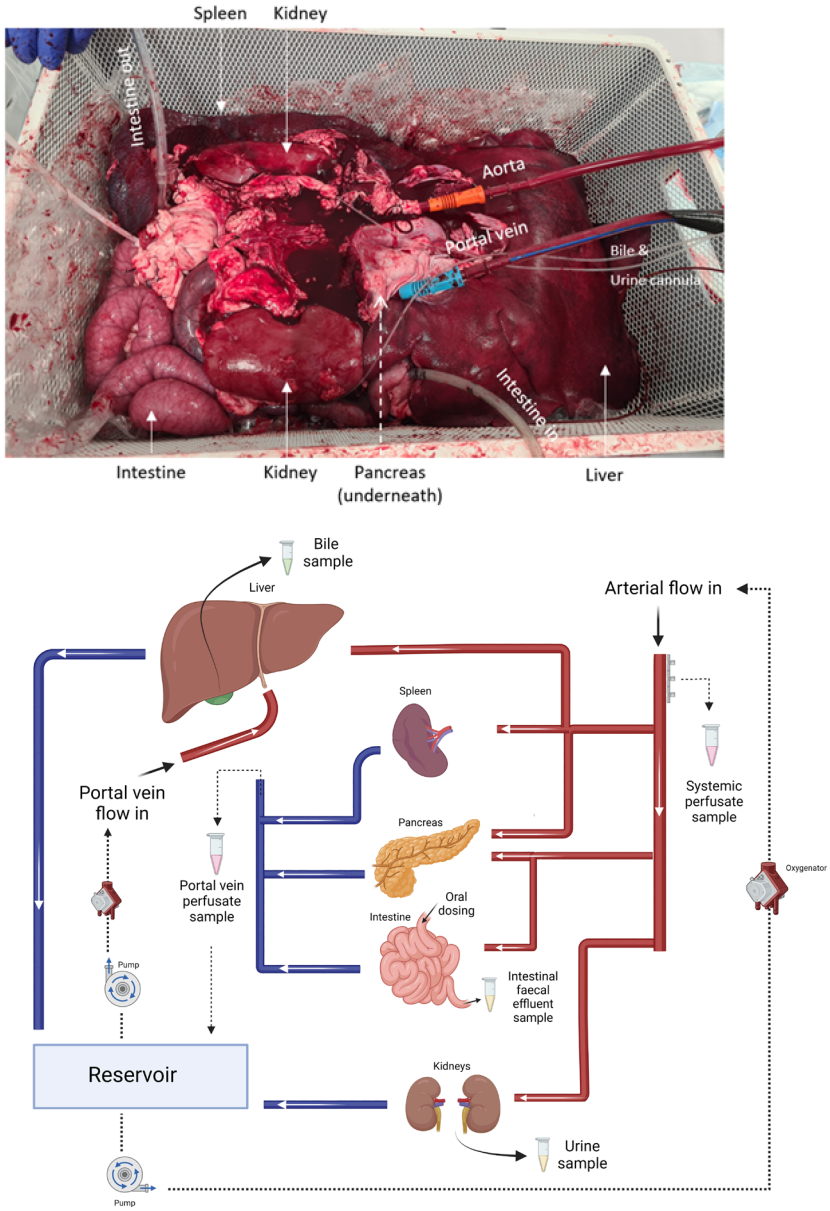

Figure 6.1 - Representation of the ex vivo perfusion model including liver, spleen, pancreas, intestine and kidneys. (A) Visual appearance of the model during normothermic machine perfusion in one of the experiments. Organs and cannulas are indicated, pancreas is indicated since it is not visible. (B) Simplified schematic representation of the gut-hepatobiliary perfusion model. Sample points are indicated by the eppendorfs including the systemic perfusate, portal vein perfusate, bile, urine and intestinal fecal effluent. Drug was dosed in the duodenum mimicking the oral dosing pathway indicated by the arrow towards the intestine 'oral dosing'.

Organ function assessment

During the perfusion experiment, blood gas analysis was executed every hour by measuring a blood gas panel, electrolytes and a hematology panel using a blood gas analyzer (iSTAT Alinity, Abbot Point of Care Inc., Princeton, NJ). Additionally, arterial and portal vein flow and resistance values were reported from the Liver Assist™ device. Next to blood gas analysis, the following parameters were measured in systemic perfusate and bile samples to study viability of the organs. Intestine: Intestinal barrier integrity was characterized by measuring FD4 and atenolol and antipyrine. FD4 was analyzed using a BioTek Synergy HT microplate reader (BioTek Instruments Inc., Winooski, VT) with an excitation/emission wavelength of 485 nm and 528 nm. FD4 concentration were determined by measuring the fluorescence in relative fluorescence units (rfu). Bioanalysis of atenolol and antipyrine is described below. Liver: lactate concentrations in the perfusate were measured by bloodgas analysis, bile production was collected in fractions and volume was measured from the collection tubes throughout the perfusion. Total bilirubin, alanine transaminase (ALT) and aspartate transaminase (AST) concentration were determined in the systemic perfusate (Reflotron-Plus system, Roche diagnostics, Almere, the Netherlands). Pancreas: C-peptide levels were measured using an ELISA (Sigma Aldrich, Zwijndrecht, the Netherlands) according to manufactures description and amylase in intestinal faecal effluent was measured (Reflotron-Plus system, Roche diagnostics, Almere, the Netherlands). Kidney: systemic perfusate sodium, potassium and blood urea nitrogen (BUN) were determined using bloodgas analysis. No assessments were performed to study the viability of the spleen.

Bioanalysis

The concentration of midazolam in systemic perfusate, portal vein perfusate, bile and tissues was quantified using LC-MS/MS (Waters, Etten-Leur, the Netherlands). Atenolol and Antipyrine in the different matrixes were measured using UPLC (Waters, Etten-Leur, the Netherlands). Perfusate, bile and tissue samples were deproteinized with acetonitrile (1:3) with the addition of 10 of µL the isotopically labelled internal standards midazolam (1 µg/mL). Thereafter samples were vortexed, centrifuged and supernatant was transferred to 96 well plate and dried under nitrogen. Samples were then dissolved in 100 µL 10% ACN + 0,1% formic acid and injected in to LC-MS/MS for quantification of midazolam, 1-OH midazolam and 1-OH midazolam glucuronide (Supplemental

Table S6.1 and S6.2) and UPLC for quantification of antipyrine and atenolol (Supplemental Table S6.3 and S6.4). Chromatograms of midazolam, atenolol and antipyrine are shown in Supplemental Figure S6.2.

Data analysis

Data obtained during the perfusion studies was analyzed using Graphpad prism version 8 (Graphpad, California, USA). Values for the area under the concentration time curve (AUC) were calculated using the linear trapezoidal method. Oral bioavailability was calculated based on F_G and F_H:

$$(1)\ F = F_a * F_G * F_H = F_a * (1 - E_G) * (1 - E_H)$$

To calculate intestinal gut-wall extraction of midazolam (E_G), midazolam metabolism into 1-OH midazolam in the intestinal lumen ($E_{G\text{-intestinal lumen}}$) and in the portal vein ($E_{G\text{-pv}}$) was calculated[3]

$$(2)\ Intestinal\ extraction\ (E_{G-intestine}) = \frac{AUC^{mdz-metab.}_{Intest.effluent}}{AUC^{mdz-metab.}_{intest.effluent} - AUC^{mdz}_{Intest.effluent}}$$

$$(3)\ Intestinal\ extraction\ (E_{G-pv}) = \frac{Q_{pv} * \left(AUC^{1-OH}_{pv} - AUC^{1-OH-calc*}_{pv}\right)}{Q_{pv} * \left(AUC^{1-OH}_{pv} - AUC^{1-OH-calc*}_{pv}\right) + Q_{pv} * \left(AUC^{mdz}_{pv} - AUC^{mdz-calc*}_{pv}\right)}$$

Where Q_{pv} is the portal vein flow, superscripts mdz and mdz-metab. refer to the parent drug and metabolites (Supplemental Figure S6.3). Subscripts pv, s and intest. effluent refer to portal vein perfusate, systemic perfusate and intestinal faecal effluent respectively. AUC represents the area under the plasma concentration time curve. To determine E_G in the portal vein, a systemic sample (without contribution of the liver is needed[3], here considered as $pv^{1\text{-mdz-calc}*}$ and $pv^{1\text{-OH-calc}*}$ (Supplemental Figure S6.3). The $AUC^{1-OH-calc*}_{pv}$ was considered the systemic circulation without liver, calculated as followed:

The portal vein - liver in concentrations of midazolam and metabolites were calculated based on FD4 measurements. Since FD4 is not metabolized by the liver, a dilution factor could be calculated based on FD4 portal vein perfusate concentration and FD4 systemic perfusate concentration. Using the FD4 data,

the pre liver in concentrations and subsequent AUC ($AUC_{pv}^{1-OH-calc*}$) was calculated.

$$(4)\ Portal\ vein^{1-OH-calc*} = \frac{Portal\ vein_{intestinal\ \ side}^{1-OH}}{\frac{FD4_{portal\ \ side}}{FD4_{systemic\ \ circulation}}}$$

Where Portal vein intestinal side sample (Supplemental Figure S6.1) is the portal vein blood flow directly coming from the intestine. The midazolam concentration in the portal vein ($AUC_{pv}^{mdz\ -calc*}$) as calculated in a similar fashion as the 1-OH concentration in the portal vein.

Fraction escaping gut wall (F_G) metabolism was defined by intestinal gut-wall extraction (E_G) of midazolam:

$$(5)\ F_G = (1 - E_G)$$

Hepatic extraction ratio (E_H) of midazolam was determined using portal vein (based on FD4 diluted calculation) and perfusate samples.

$$(6)\ Hepatic\ extraction\ (E_H) = \frac{Conc.midazolam_{pv}^{mdz\ -calc*} - Conc.midazolam_{systemic\ \ circulation}}{Conc.midazolam_{pv}^{mdz\ -calc*}}$$

Based on the hepatic extraction ratio, the fraction escaping hepatic elimination could be calculated:

$$(7)\ F_H = (1 - E_H)$$

Results

Organs show proper viability and function during perfusion

Figure 6.2A - N show organ specific viability and injury markers for the intestine, liver, pancreas and kidney. The intestinal barrier function was assessed by measuring the permeability FD4 and of atenolol, and antipyrine. Varying but high levels of FD4 were collected from the intestinal faecal effluent ($1.2*10^8 \pm 1.0*10^8$ rfu/mL perfusate) while detection of FD4 in the portal vein perfusate and systemic perfusate remained low ($0.03*10^8 \pm 0.03*10^8$ rfu/mL perfusate vs $0.02*10^8 \pm 0.02*10^8$ rfu/mL perfusate respectively) indicating

minimal leakage of FD4 into the perfusate and thus a proper intestinal barrier (Figure 6.2A). Besides FD4, the permeability of atenolol and antipyrine was measured. Atenolol has a moderately permeability and translocates via the paracellular route while antipyrine is a high permeable drug which translocates via the transcellular route. Atenolol was, on average, detected at slightly lower concentrations in the portal vein perfusate compared to antipyrine (Supplemental Figure S6.4), indicating proper preservation of transcellular and paracellular transport routes (Figure 6.2B-C). Additionally, intestinal peristalsis was observed in all experiments between 30-120 min after start of the perfusion and intestinal peristalsis remained throughout the whole length of the experiment (Supplemental Video S6.1). Regarding liver viability, lactate levels showed to remain stable throughout the perfusion with a small decline observed for 2 out of 4 experiments (Figure 6.2D). Figure 6.2E shows the bile production of the livers. Bile production was very consistent throughout the perfusion time with an average bile production of 148.42±36.81 mL after 420 min of perfusion. ALT and AST increased 60 min after starting perfusion and remained stable throughout the perfusion (Figure 6.2F-G). Bilirubin showed to be very stable in experiment 3 and 4 (9.1 and 9.3 µmol/L respectively), however in experiment 1 and 2, increase in perfusate bilirubin was observed (23.1 and 35 µmol/L respectively at t=420 min) (Figure 6.2H). As a marker of endocrine and exocrine pancreas viability, C-peptide secretion and intestinal amylase concentration were measured in systemic perfusate and intestinal faecal effluent respectively. C-peptide was detected in the systemic perfusate in all experiments at t=60 min with a concentration of 8.47±1.38 ng/mL and remained stable throughout the whole perfusion (Figure 6.2I). The intestinal faecal effluent showed to contain high concentrations of amylase (AUC 49472 ±17565 U/L) indicating active secretion by the pancreas (Figure 6.2J). Figure 6.2K demonstrates the glucose kinetics during organ perfusion. In two the of the multi-organ perfusion studies (study 1 and 4) stable glucose levels throughout the perfusion were observed with a maximum glucose peak of 11mmol/L at 30 min indicating possible glucose regulation by the pancreas. The other perfusions showed a peak glucose levels of ~39 mmol/L 60 min after perfusion, whereafter linear glucose uptake was observed indicating glucose consumption by the various organs. In the absence of a kidney function biomarker, systemic perfusate levels of sodium, potassium and blood urea nitrogen (BUN) were measured (Figure 6.2L-N). Sodium and potassium levels remained stable throughout the perfusion duration and minimally increased, indicating maintenance of a proper biochemical environment. BUN increased

during the perfusion reaching a final concentration of 38.75±5.90 mmol/L at 420 min of perfusion, retaining relatively low levels of perfusate BUN levels to single organ perfusion (Supplemental Figure S6.5). Minimal urine output (0-10 mL) was observed during perfusion. Together, these data shown proper viability as well as functionality up to 420 min of perfusion of different organs involved in the perfusion model (Supplemental Figure S6.6).

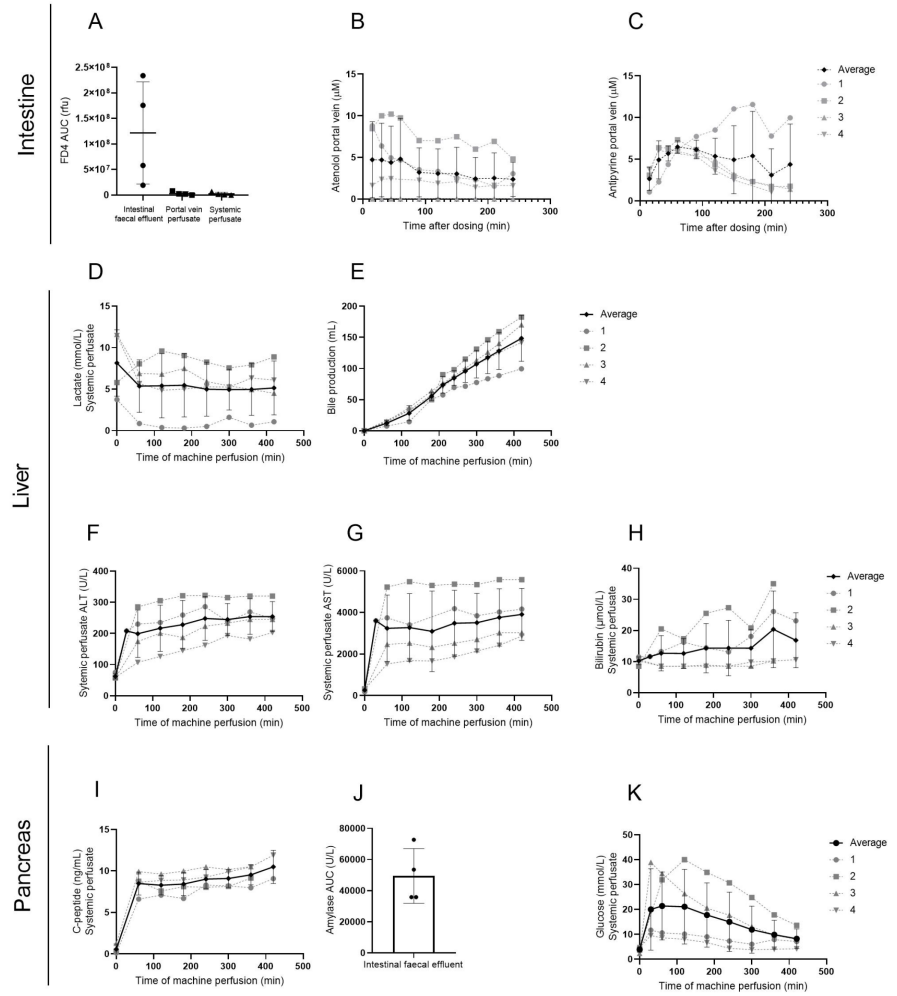

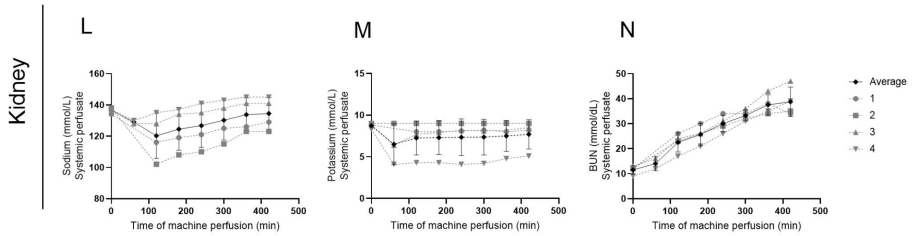

Figure 6.2 - General viability, functionality and injury markers of the intestine (A-C), liver (D-H), pancreas (I-J) and kidney (L-M). (A) Area under the curve (AUC) of FD4 measured in the intestinal faecal effluent, portal vein perfusate and systemic perfusate. (B-C) Concentration of Atenolol and Antipyrine measured in the portal vein perfusate as markers for paracellular and transcellular transport respectively. (D) systemic perfusate lactate concentration (E) cumulative bile production during 420 min of perfusion, (F) ALT concentration measured in the systemic perfusate, (G) AST concentration measured in the systemic perfusate, (H) bilirubin concentration measured in the systemic perfusate. (I) C-peptide concentration was measured in the systemic perfusate, (J) AUC of amylase measured in the intestinal fecal effluent and (K) systemic perfusate glucose concentrations . (L) Systemic perfusate levels of sodium (M) Systemic perfusate levels of potassium and (n) systemic perfusate levels of BUN. Data represents mean ± SD of 4 individual experiments. Individual experiments are presented by the dotted lines.

Active midazolam absorption, metabolism and excretion

Absorption and metabolism of midazolam was studied to characterize the viability of the intestine and liver. Figure 6.3A-C illustrate the role of the intestine (and liver) in midazolam metabolism. After an intraduodenal dose, midazolam was detected in the portal vein perfusate to a higher extent than the systemic perfusate indicating active midazolam absorption. The C_{max} concentration in the portal vein was 426.47 nM, 90 min after administration. Corresponding C_{max} in systemic perfusate was 80.16 nM at 90 min after administration. Portal vein concentration decreased over time to 117.60 nM at 240 min after dosing, with a perfusate concentration of 36.01 nM. Figure 6.3B shows the 1-OH midazolam concentrations in the portal vein and systemic perfusate. 1-OH midazolam concentrations showed to be higher in the portal vein compared to the perfusate indicating active gut wall metabolism of midazolam to its metabolite. Samples from the intestinal faecal effluent were taken to assess midazolam and metabolite concentrations (Figure 6.3C). Midazolam was detected at higher levels compared to the metabolites 1-OH midazolam and 1-OH midazolam glucuronide (2889±2321 vs. 111.59±86.22 vs. 1.31±1.06 µM/0-240min respectively) showing incomplete absorption of midazolam as well as gut-wall metabolism and interestingly, excretion to the luminal side. Figure 6.3D and 6.33E demonstrates the liver contribution to the metabolism of midazolam. 1-

OH midazolam glucuronide was measured at slightly higher levels in the systemic perfusate compared to the portal vein perfusate. Biliary excretion of midazolam was demonstrated with a C_{max} at 90 min (46.78 ng), and total biliary excretion of 0.04% (±0.01%) of the administered dose. The metabolite 1-OH midazolam glucuronide was also detected in the bile, however only in 1 out of 4 experiments, at minimal output (0.02% of administered dose). Figure 6.3F shows the systemic midazolam profile. The metabolite, 1-OH midazolam was detected in the perfusate 30 min after dosing and linearly increased throughout the perfusion with a C_{max} of 57.20 nM at 210 min whereafter a decrease was observed. The midazolam metabolite 1-OH midazolam glucuronide was detected in the perfusate 30 min after perfusion. The glucuronide demonstrated a more rapid increase in its detection in the systemic perfusate over time (117.99 nM at 240 min) compared to 1-OH midazolam. The relative slight increase in the detection of 1-OH midazolam with the steep increase in the detection of 1-OH glucuronide suggest metabolism of 1-OH into its glucuronide.

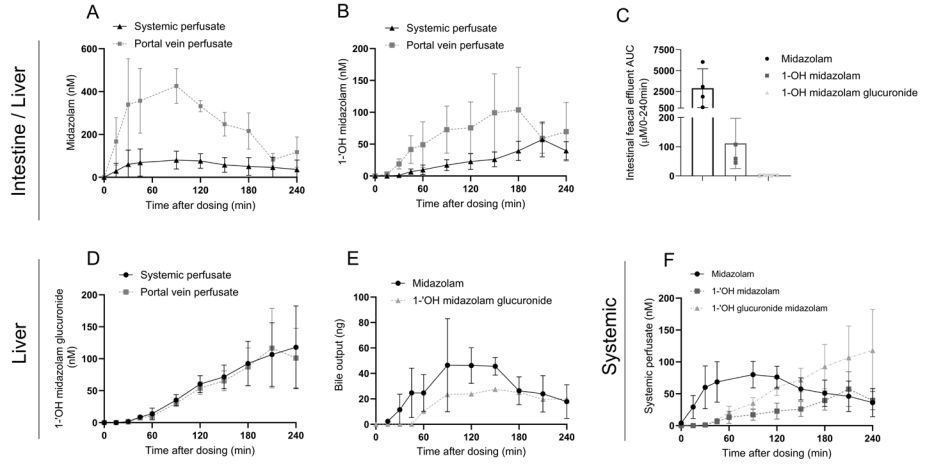

Figure 6.3 - Midazolam absorption, metabolism and elimination categorized for the contribution of the intestine/liver (A-C), liver (D-E and systemic profile (F) measured in the ex vivo perfusion model after duodenal administration of 20mg midazolam. Intestinal absorption and metabolism is shown in: (A) midazolam concentration in the systemic and portal vein perfusate (B) 1-OH midazolam concentration in the systemic and portal vein perfusate and (C) midazolam, 1-OH midazolam and 1-OH midazolam glucuronide concentrations (AUC) detected in the intestinal faecal effluent. Liver metabolism and elimination is shown in: (D) 1-OH midazolam glucuronide in the systemic and portal vein perfusate, (E) biliary elimination of midazolam and 1-OH midazolam glucuronide and (F) midazolam, 1-OH midazolam and 1-OH midazolam glucuronide PK profile measured in the systemic perfusate. Data represents mean ± SD of 4 individual experiments.

High tissue levels of midazolam in the intestine

The concentration of midazolam, 1-OH midazolam and 1-OH midazolam glucuronide after 240 min of perfusion were determined in intestine, liver and kidney tissue (Figure 6.4A-B). Concentration of 1-OH midazolam showed to be below the limit of quantification in all the organs. Compared to kidney (0.12±0.08 nM/mg tissue) and liver (0.10±0.03 nM/mg tissue), high concentrations of midazolam were observed in the intestine (5.20±3.97 nM/mg tissue) (Figure 6.4A). The conjugated metabolite, 1-OH midazolam glucuronide, tended to show higher tissue levels in the liver (0.06±0.08 nM/mg tissue) compared to intestine (0.02±0.01 nM/mg tissue) and kidney (0.03±0.02 nM/mg tissue). However this was mainly observed in 1 out of 3 studies.

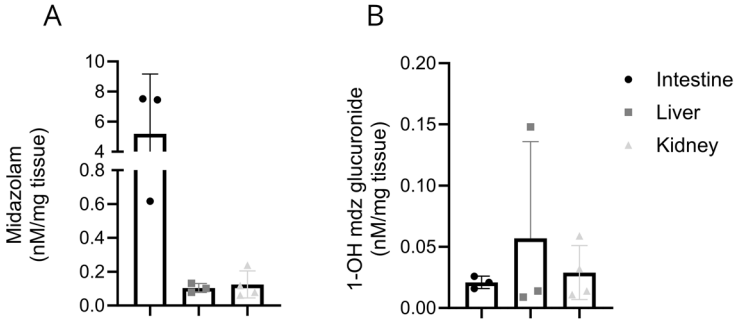

Figure 6.4 - Tissue concentrations of midazolam and 1-OH midazolam glucuronide measured at the end of the perfusion in the ex vivo perfusion model after duodenal administration of 20mg midazolam. (A) tissue concentration of midazolam and (B) tissue concentration of 1-OH midazolam glucuronide in intestine (n=3), liver (n=3) and kidney (n=4). Data represents mean ± SD of 3-4 individual experiments. Multiple biopsies per experiment were taken (n=2-3)

Determination of the oral bioavailability

Based on the measured concentrations in the perfusate, portal vein and intestinal lumen the E_H, E_G, F_G, F_H and subsequently F_{oral} was calculated. The E_G, metabolite formation to the gut lumen showed to be less than the metabolite formation in the portal vein (0.051±0.03 vs. 0.16±0.10 respectively). Together, an E_G of 0.21±0.11 was measured in our model (Figure 6.5A). The E_H varied between 0.55-0.74 with an average of 0.65±0.07. The F_G and F_H showed a value of 0.78±0.11 and 0.35±0.07 respectively, indicating more extensive hepatic metabolism than through intestinal metabolism. Assuming a fraction absorbed of 1, the F_{oral} was calculated to be 0.27±0.05.

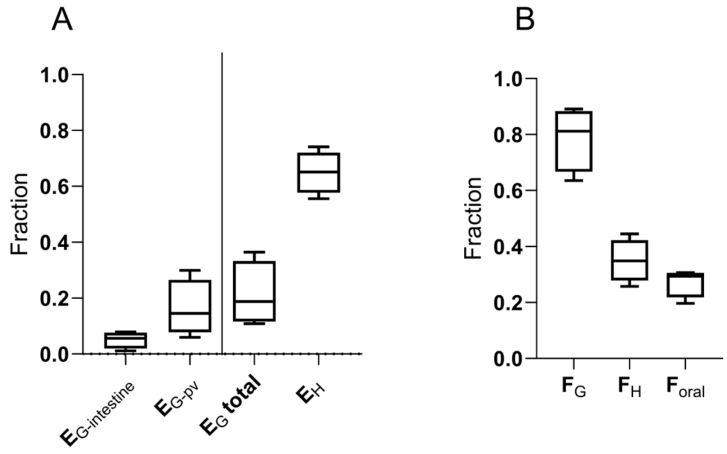

Figure 6.5 - Oral bioavailability of midazolam (A) Gut wall extraction of midazolam, determined in the intestinal faecal effluent (E_G-intestine), portal vein and systemic perfusate (E_G-pv), combined showing the E_G total, and hepatic extraction of midazolam measured in the portal vein and systemic perfusate. (B) Fraction escaping gut wall metabolism, fraction escaping hepatic extraction and oral bioavailability of midazolam. Data represents mean ± SD of 4 individual experiments.

Discussion

To date, complete ADME profiles with a focus on oral bioavailability can only be studied in *in vivo* models as it remains difficult to recapitulate all organ functions within a single *in vitro* model. However, with the innovations into state-of-the-art perfusion devices we have demonstrated the ability to perfuse multiple abdominal organs *en bloc* in an *ex vivo* setting. The model showed a stable flow, intestinal peristalsis was observed throughout the experiment and viability of the organs was demonstrated by bloodgas analysis, specific viability assays and by showing absorption, metabolism and excretion of midazolam.

Although *ex vivo* NMP is typically conducted with a single organ, the simultaneous perfusion of multiple organs occurs less frequently. Our data indicates that the inclusion of multiple homeostatic organs (e.g. liver, kidneys and pancreas) holds significant advantages, especially in maintaining the acid-base balance and glucose regulation of the perfusate. This is also observed by Chung et al.,[15,19] and He et al.,[16] showing the addition of a kidney to the liver circuit improved the biochemical environment. During liver perfusion, a spike in glucose concentration is typical[20]. Interestingly, in two out of four perfusions

only a slight increase occurred. We hypothesize that the addition of the pancreas to the circuit was beneficial for the glucose regulation and homeostasis, as evidenced by a concurrent production of C-peptide. Moreover, no additional glucose infusion was needed, suggesting effective glucose regulation by the pancreas. Delayed warm-up of organs in two of the perfusions might explain the glucose rise at t=60 min, affecting the pancreas functionality and viability. Using a multi-organ perfusion approach, including homeostatic organs, achieving prolonged perfusion will become more feasible. Previous studies demonstrated prolonged abdominal organ perfusion, with viability up to 24 hours[21] and 45 hours[18]. Both above mentioned studies used organs obtained before sacrificing the animal, allowing for minimal warm ischaemic time before preservation. To our knowledge, no other previous studies demonstrated a multi-organ model using slaughterhouse organs, in which warm ischemia times are inherent. With this study we show the possibility to use slaughterhouse material (waste material), contributing to the 3R principle of reduction in the use of animal testing[22]. Additionally, the availability of slaughterhouse organs is a significant advantage allowing for experimentation without the need for an animal laboratory[23]. However, good agreements with the slaughterhouse is essential to ensure proper quality of the organs during resection of the *en bloc* organs out of the carcass. The complexities encountered in small intestinal and multivisceral organ transplantation show similarities to our developed *ex vivo* model[24]. We observed extensive fluid secretion into the small intestines. It is known that the small intestine secretes 8-9 liters water including electrolytes per day which is reabsorbed by the ileum and the colon tissue[25,26]. Extensive excretion is a phenomena known in small intestine transplantation; colectomy patients suffer from severe diarrhea after surgery indicating the inability to reabsorb the secreted fluid. Furthermore, in a rat intestine-transplant model obtained after circulatory death, abnormalities were shown in intestinal secretion[27,28]. Also Pang et al.[29] reported the hypersecretion into the lumen of the intestine in a gut-liver in situ rat perfusion model, however this could be overcome by the infusion of norepinephrine and dexamethasone. This strategy limiting hypersecretion is promising for future multi-organ experiments and would possibly enable to include the whole small intestine allowing for even better absorption studies.

To demonstrate the applicability of the perfusion model to study the first pass effect and oral bioavailability, the metabolism of midazolam was studied. Since

midazolam is metabolized by the intestine as well as the liver by CYP3A in both of these organs, valuable insight can be generated regarding the extent of involvement of the organs into the first-pass metabolism. Intestinal absorption of midazolam was observed followed by detection of 1-OH midazolam and 1-OH midazolam glucuronide in the portal vein and systemic perfusate indicating CYP3A metabolism and UGT1A4 and UGT2B4/2B7 activity in the intestine and liver. Additionally, the presence of these metabolites in the intestinal faecal effluent suggest gut wall metabolism and intestinal glucuronidation to some extent. High levels of 1-OH midazolam in the portal vein perfusate indicate gut-wall metabolism, while extensive hepatic glucuronidation was observed. This was evidenced by increasing levels of the glucuronide in the systemic perfusate assuming a higher expression of UGT enzymes in the liver compared to intestinal UGT expression. Minor urine excretion was observed during the perfusion and thus urinary elimination of midazolam and the metabolites could not be studied. We hypothesize that the limited urine production could be due to perfusate conditions, ischemia reperfusion injury or the water flux from the perfusate to the intestinal lumen, limiting the 'need' to produce urine for the kidneys.

The hepatic extraction ratio calculated in the multi-organ model showed to be 0.65 (±0.07). Although minor to no hepatic extraction data of midazolam in pigs is known, the reported human hepatic extraction ratio showed to be slightly lower (0.44±0.14)[30]. Midazolam extraction is affected by the blood flow and the activity of metabolizing enzymes[31]. Multiple studies have demonstrated that porcine liver microsomes possess a higher CYP3A4 activity compared to human liver microsomes[32,33]. Also our lab demonstrated a higher activity of porcine liver microsomes compared to human liver microsomes (Supplemental Figure S6.7). A higher activity of CYP3A can result in a higher hepatic extraction ratio and thus a higher first-pass effect, confirming the results observed in our perfusion model. Ochs et al.,[34] demonstrated the intestinal and hepatic extraction of midazolam in pigs by comparing oral administration versus iv administration. The systemic venous / portal venous ratio of midazolam showed to be 0.15 indicating extensive hepatic extraction. IV administration showed almost similar AUC values in systemic venous and portal venous samples suggesting minimal intestinal extraction. This study showed that the extraction of midazolam after duodenal administration could be contributed to almost entirely hepatic metabolism. In humans, intestinal extraction plays a more dominant role since extraction values of 0.43-0.44 have been reported

for the intestine, indicating substantial involvement of the intestine in the extraction process[3,30]. Thummel et al.,[30] demonstrated a large variation within the intestinal extraction (0.0–0.77), as also shown by Brill et al.,[35] predicting extraction values between 0.05–0.8 in morbidly obese patients. One possible explanation for the disparity in observed intestinal extraction data between humans and pigs could be variations in the abundance of CYP3A4 enzymes. Schelstraete et al.,[36] compared the CYP450 enzymatic status in porcine livers and intestine to human enzymatic status. Duodenal relative quantitative results showed to be remarkably similar between pigs and men (CYP3A4 88% in pig vs 82% in humans). However, intestinal CYP450 microsomal activity was significantly lower in porcine microsomes for CYP3A, even up to 6-10 times lower as reported in human[37]. Subsequently, the overall oral bioavailability showed to be 27% in our model. Only two *in vivo* studies using pigs (micro minipigs and Gottinger minipigs) reported the bioavailability of midazolam after oral intake, showing values between 3.0% and 14%[32,34,38]. Although our reported oral bioavailability data is close to the reported *in vivo* data, slight underprediction of the intestinal metabolism in our model could affect the F_G and thus affect the oral bioavailability. The slight underprediction of the intestinal metabolism could be due to the inclusion of only ~2 meter of small intestinal tissue. Although the highest expression of CYP3A4 is detected in the duodenum and gradually decreases along the intestinal tract, metabolism further along the intestine could have contributed to a higher intestinal metabolism[3,39-41]. Moreover, temperature of the ex vivo organs might have influenced the metabolism of midazolam. Despite maintaining the perfusate temperature at 38°C which was monitored at the arterial and venous flow, the ex vivo organs placed in a box were susceptible to cooling down. This could result in lower tissue temperature that could have impacted the (intestinal) absorption and metabolism of midazolam and be a reason for variation in the results[42,43]. Besides detection of 1-OH midazolam and 1-OH midazolam glucuronide, we observed multiple hydroxy and glucuronide metabolites (Supplemental Figure S6.8) however, not quantified. This could also partly account for the slight underprediction of metabolism. Also differences in pig species used in these studies compared to our study can affect the F_G and F_H and thus affect the oral bioavailability. Clinical studies using human subjects show a higher midazolam bioavailability; between 29-44%[3,30,44]. Taking into account the higher CYP3A4 activity in the liver in pig studies, human *in vivo* studies show lower F_H values resulting in a higher oral bioavailability which is in line with our data. In summary, the generated hepatic and intestinal extraction

data is in line with *in vivo* pig data. To translate this data to humans, the use of physiologically based pharmacokinetic (PBPK) modeling with allometric scaling could be applied. Multiple pig PBPK models have been developed since there is a growing use of pigs as preclinical species[45]. On the other hand, multi-organ perfusions can generate novel insights and input for these PBPK modelling exercises. One of the challenges in PBPK modeling is to dissect out the contributions of the intestines and liver, two serially arranged organs in first-pass metabolism[46]. Studying PK processes of organs involved in ADME in an isolated environment gives the ability to control the process. The ability to take (unlimited) samples from different locations (e.g. different venous outflows) and tissues over time can generate valuable information regarding the contribution of each organ into the metabolism of a drug. Especially sampling from the intestinal faecal effluent and the portal venous blood generating insight into gut-wall metabolism is very unique. The model presents numerous future perspectives; it offers the potential for studying regional absorption as the expression of transporters like Pgp, OATP and CYP enzymes varies along the intestinal tract[47]. Since the model closely resembles physiology, including intact intestinal tissue and peristalsis the model could be used to study formulation effects since sampling from the intestinal faecal effluent and portal venous blood stream is feasible and dosing at a physiological pH can be applied as the tissue is able to handle the enzymatic and pH environment. A pre-digestion protocol designed to mimick stomach digestion can even more accurately stimulate gastrointestinal conditions, thus better simulate in vivo conditions. This is particularly important as the stomach's acidic environment aids in solubilizing and dissolving drugs[48]. Furthermore, the gut-hepatobiliary model offers an excellent opportunity to study drug-drug interactions (DDI) as DDI can occur at the intestinal as well as the hepatic level as currently a combination of both models is needed in order to properly predict the magnitude of DDI.

Conclusion

We have successfully developed a porcine *ex vivo* perfusion model of multiple abdominal organs and demonstrated its capabilities and potential use in studying ADME processes. Using this model we were able to characterize pre-systemic extraction of midazolam by measuring the intestinal as well as hepatic extraction. As a result, oral bioavailability could be determined. $F_{H,}$ F_G and oral bioavailability findings were in line with pig *in vivo* data. This model,

complemented with physiologically based pharmacokinetic modelling is a valuable approach to investigate the first-pass effect and oral bioavailability of novel pharmaceutical compounds. By employing this approach, valuable insights can be generated into the absorption and metabolism of new drugs, thereby facilitating the development and optimization of drug candidates for human use.

Acknowledgement

We thank Arjan de Vries, Ioana Barbu, Esmeé Wierenga and Kevin Weijgertse with the help of bioanalysis of midazolam, antipyrine and atenolol. We thank Timo Eijkman for the assistance with the preparation of organs prior to perfusion. We thank Aswin Mencke for the histopathological analysis.

References

1. Alqahtani S, Mohamed LA, Kaddoumi A. Experimental models for predicting drug absorption and metabolism. Expert Opinion on Drug Metabolism & Toxicology 2013;9:1241-1254.
2. Varma MV, Obach RS, Rotter C, Miller HR, Chang G, Steyn SJ, El-Kattan A, et al. Physicochemical space for optimum oral bioavailability: contribution of human intestinal absorption and first-pass elimination. Journal of medicinal chemistry 2010;53:1098-1108.
3. Paine MF, Shen DD, Kunze KL, Perkins JD, Marsh CL, McVicar JP, Barr DM, et al. First-pass metabolism of midazolam by the human intestine. Clinical Pharmacology & Therapeutics 1996;60:14-24.
4. Peters SA, Jones CR, Ungell A-L, Hatley OJ. Predicting drug extraction in the human gut wall: assessing contributions from drug metabolizing enzymes and transporter proteins using preclinical models. Clinical pharmacokinetics 2016;55:673-696.
5. Heikkinen AT, Baneyx G, Caruso A, Parrott N. Application of PBPK modeling to predict human intestinal metabolism of CYP3A substrates–an evaluation and case study using GastroPlus™. European journal of pharmaceutical sciences 2012;47:375-386.
6. Eshmuminov D, Becker D, Bautista Borrego L, Hefti M, Schuler MJ, Hagedorn C, Muller X, et al. An integrated perfusion machine preserves injured human livers for 1 week. Nature biotechnology 2020;38:189-198.
7. Hamed M, Barlow A, Dolezalova N, Khosla S, Sagar A, Gribble F, Davies S, et al. Ex vivo normothermic perfusion of isolated segmental porcine bowel: a novel functional model of the small intestine. BJS open 2021;5:zrab009.
8. Nicholson M, Hosgood S. Renal transplantation after ex vivo normothermic perfusion: the first clinical study. American Journal of Transplantation 2013;13:1246-1252.
9. Ogbemudia AE, Hakim G, Dengu F, El-Gilani F, Dumbill R, Mulvey J, Sayal K, et al. Development of ex situ normothermic reperfusion as an innovative method to assess pancreases after preservation. Transplant International 2021;34:1630-1642.
10. Clark T, Bau L, Dengu F, Voyce D, Carlisle R, Friend P, Coussios C. Predicting clinical pharmacokinetics and toxicity of current and emerging oncology therapeutics by normothermic perfusion of isolated human-sized organs. Cancer Research 2021;81: 1369-1369.
11. Posma RA, Venema LH, Huijink TM, Westerkamp AC, Wessels AMA, De Vries NJ, Doesburg F, et al. Increasing metformin concentrations and its excretion in both rat and porcine ex vivo normothermic kidney perfusion model. BMJ Open Diabetes Research and Care 2020;8:e000816.
12. Stevens LJ, Dubbeld J, Doppenberg JB, van Hoek B, Menke AL, Donkers JM, Alsharaa A, et al. Novel explanted human liver model to assess hepatic extraction, biliary excretion and transporter function. Clinical Pharmacology & Therapeutics 2023;114(1):137-147.
13. Stevens LJ, Zhu AZ, Chothe PP, Chowdhury SK, Donkers JM, Vaes WH, Knibbe CA, et al. Evaluation of normothermic machine perfusion of porcine livers as a novel preclinical model to predict biliary clearance and transporter-mediated drug-drug interactions using statins. Drug Metabolism and Disposition 2021;49:780-789.
14. Rowland M, Benet LZ, Graham GG. Clearance concepts in pharmacokinetics. Journal of pharmacokinetics and biopharmaceutics 1973;1:123-136.
15. Chung WY, Gravante G, Al-Leswas D, Arshad A, Sorge R, Watson CC, Pollard C, et al. The development of a multiorgan ex vivo perfused model: results with the porcine liver-kidney circuit over 24 hours. Artificial Organs 2013;37:457-466.
16. He X, Ji F, Zhang Z, Tang Y, Yang L, Huang S, Li W, et al. Combined liver-kidney perfusion enhances protective effects of normothermic perfusion on liver grafts from donation after cardiac death. Liver Transplantation 2018;24:67-79.
17. Li J, Jia J, He N, Jiang L, Yu H, Li H, Peng Y, et al. Combined kidney-liver perfusion enhances the proliferation effects of hypothermic perfusion on liver grafts via upregulation of IL-6/Stat3 signaling. Molecular medicine reports 2019;20:1663-1671.

18. Chen C, Chen M, Lin X, Guo Y, Ma Y, Chen Z, Ju W, et al. En bloc procurement of porcine abdominal multiple organ block for ex situ normothermic machine perfusion: a technique for avoiding initial cold preservation. Annals of Translational Medicine 2021;9(14):1116.
19. Chung WY, Gravante G, Al-Leswas D, Alzaraa A, Sorge R, Ong SL, Pollard C, et al. The autologous normothermic ex vivo perfused porcine liver-kidney model: improving the circuit's biochemical and acid-base environment. The American journal of surgery 2012;204:518-526.
20. Watson CJ, Jochmans I. From "gut feeling" to objectivity: machine preservation of the liver as a tool to assess organ viability. Current transplantation reports 2018;5:72-81.
21. Chien S, Diana JN, Oeltgen PR, Todd EP, O'Connor WN, Chitwood Jr WR. Eighteen to 37 hours' preservation of major organs using a new autoperfusion multiorgan preparation. The Annals of thoracic surgery 1989;47:860-867.
22. Han JJ. FDA Modernization Act 2.0 allows for alternatives to animal testing. In: Wiley Online Library; 2023.
23. Dengu F, Neri F, Ogbemudia E, Ebeling G, Knijff L, Rozenberg K, Dumbill R, et al. Abdominal multiorgan procurement from slaughterhouse pigs: A bespoke model in organ donation after circulatory death for ex vivo organ perfusion compliant with the 3 Rs (reduction, replacement & refinement). Annals of translational medicine 2022;10(1).
24. Abu-Elmagd KM, Costa G, Bond GJ, Soltys K, Sindhi R, Wu T, Koritsky DA, et al. Five hundred intestinal and multivisceral transplantations at a single center: major advances with new challenges. Annals of surgery 2009;250:567-581.
25. Donohoe CL, Reynolds JV. Short bowel syndrome. The surgeon 2010;8:270-279.
26. Field M. Intestinal secretion. Gastroenterology 1974;66:1063-1084.
27. Goulet O, Colomb-Jung V, Joly F. Role of the colon in short bowel syndrome and intestinal transplantation. Journal of pediatric gastroenterology and nutrition 2009;48:S66-S71.
28. Teitelbaum DH, Sonnino RE, Dunaway DJ, Stellin G, Harmel RP. Rat jejunal absorptive function after intestinal transplantation: effects of extrinsic denervation. Digestive diseases and sciences 1993;38:1099-1104.
29. Pang KS, Cherry W, Ulm E. Disposition of enalapril in the perfused rat intestine-liver preparation: absorption, metabolism and first-pass effect. Journal of Pharmacology and Experimental Therapeutics 1985;233:788-795.
30. Thummel KE, O'Shea D, Paine MF, Shen DD, Kunze KL, Perkins JD, Wilkinson GR. Oral first-pass elimination of midazolam involves both gastrointestinal and hepatic CYP3A-mediated metabolism. Clinical Pharmacology & Therapeutics 1996;59:491-502.
31. Dundee J, Collier P, Carlisle R, Harper K. Prolonged midazolam elimination half-life. British journal of clinical pharmacology 1986;21:425-429.
32. Mogi M, Toda A, Iwasaki K, Kusumoto S, Takehara H, Shimizu M, Murayama N, et al. Simultaneous pharmacokinetics assessment of caffeine, warfarin, omeprazole, metoprolol, and midazolam intravenously or orally administered to Microminipigs. The Journal of toxicological sciences 2012;37:1157-1164.
33. Thörn HA, Lundahl A, Schrickx JA, Dickinson PA, Lennernäs H. Drug metabolism of CYP3A4, CYP2C9 and CYP2D6 substrates in pigs and humans. European journal of pharmaceutical sciences 2011;43:89-98.
34. Ochs H, Greenblatt D, Eichelkraut W, Bakker C, Göbel R, Hahn N. Hepatic vs. gastrointestinal presystemic extraction of oral midazolam and flurazepam. Journal of Pharmacology and Experimental Therapeutics 1987;243:852-856.
35. Brill MJ, Välitalo PA, Darwich AS, van Ramshorst B, Van Dongen H, Rostami–Hodjegan A, Danhof M, et al. Semiphysiologically based pharmacokinetic model for midazolam and CYP3A mediated metabolite 1-OH-midazolam in morbidly obese and weight loss surgery patients. CPT: pharmacometrics & systems pharmacology 2016;5:20-30.
36. Schelstraete W, Clerck L, Govaert E. Characterization of porcine hepatic and intestinal drug metabolizing CYP450. comparison with human orthologues from A quantitative, activity and selectivity perspective 2019;2019:9.

37. Galetin A, Houston JB. Intestinal and hepatic metabolic activity of five cytochrome P450 enzymes: impact on prediction of first-pass metabolism. Journal of Pharmacology and Experimental Therapeutics 2006;318:1220-1229.
38. Lignet F, Sherbetjian E, Kratochwil N, Jones R, Suenderhauf C, Otteneder MB, Singer T, et al. Characterization of pharmacokinetics in the Göttingen minipig with reference human drugs: an in vitro and in vivo approach. Pharmaceutical research 2016;33:2565-2579.
39. Berggren S, Gall C, Wollnitz N, Ekelund M, Karlbom U, Hoogstraate J, Schrenk D, et al. Gene and protein expression of P-glycoprotein, MRP1, MRP2, and CYP3A4 in the small and large human intestine. Molecular pharmaceutics 2007;4:252-257.
40. Bruyere A, Decleves X, Bouzom F, Ball K, Marques C, Treton X, Pocard M, et al. Effect of variations in the amounts of P-glycoprotein (ABCB1), BCRP (ABCG2) and CYP3A4 along the human small intestine on PBPK models for predicting intestinal first pass. Molecular pharmaceutics 2010;7:1596-1607.
41. Nishi K, Ishii T, Wada M, Amae S, Sano N, Nio M, Hayashi Y. The expression of intestinal CYP3A4 in the piglet model. In: Transplantation proceedings; 2004: Elsevier; 2004:361-363.
42. Tortorici MA, Kochanek PM, Poloyac SM. Effects of hypothermia on drug disposition, metabolism, and response: a focus of hypothermia-mediated alterations on the cytochrome P450 enzyme system. Critical care medicine 2007;35:2196-2204.
43. van den Broek MP, Groenendaal F, Egberts AC, Rademaker CM. Effects of hypothermia on pharmacokinetics and pharmacodynamics: a systematic review of preclinical and clinical studies. Clinical pharmacokinetics 2010;49:277-294.
44. Allonen H, Ziegler G, Klotz U. Midazolam kinetics. Clinical Pharmacology & Therapeutics 1981;30:653-661.
45. Henze LJ, Koehl NJ, O'Shea JP, Kostewicz ES, Holm R, Griffin BT. The pig as a preclinical model for predicting oral bioavailability and in vivo performance of pharmaceutical oral dosage forms: a PEARRL review. Journal of pharmacy and pharmacology 2019;71:581-602.
46. Pang KS, Yang QJ, Noh K. Unequivocal evidence supporting the segregated flow intestinal model that discriminates intestine versus liver first-pass removal with PBPK modeling. Biopharmaceutics & Drug Disposition 2017;38:231-250.
47. Vaessen SF, van Lipzig MM, Pieters RH, Krul CA, Wortelboer HM, van de Steeg E. Regional expression levels of drug transporters and metabolizing enzymes along the pig and human intestinal tract and comparison with Caco-2 cells. Drug metabolism and disposition 2017;45:353-360.
48. Mitra A, Kesisoglou F. Impaired drug absorption due to high stomach pH: a review of strategies for mitigation of such effect to enable pharmaceutical product development. Molecular pharmaceutics 2013;10:3970-3979.

Supplementary materials

Table S6.1 - Details of the LC/MS conditions; Quantification of masses and retention times.

Compound	Rt (min)	Exact mass	Polarity	Fragment	m/z
Midazolam	14.81	326.0855	Positive	tbd	tbd
1-OH midazolam	16.66	342.0804	Positive	tbd	tbd
1-OH midazolam glucuronide	10.36	518.1125	Positive	tbd	tbd

Table S6.2 - Details of the LC/MS conditions used for the analysis midazolam and metabolites.

Compound	Column	Mobile Phase A	Mobile Phase B	Time (min)	Mobile Phase A (%)	Mobile Phase B (%)	Flow (mL/min)
Midazolam	Waters Acquity	5mM	Acetonitrile	0	100	0	0.4
1-OH	HSS-c18(100 x 2.1	ammonium		1.11	85	15	
midazolam	mm i.d., 1.8 µm),	formate in		16.00	75	25	
(glucuronide)	serial no.	water pH		16.50	0	100	
	#01593022418354	4.0		20.00	0	100	

Table S6.3 - Details of the UPLC conditions; Quantification of masses and retention times of atenolol and antipyrine.

Compound	Rt (min)	Exact mass	Polarity
Atenolol	3.81	266.336	positive
Antipyrine	7.01	188.226	positive

Table S6.4 - Details of the UPLC conditions used for the analysis atenolol and antipyrine.

Compound	(pre) Column	Mobile Phase A	Mobile Phase B	Time (min)	Mobile Phase A (%)	Mobile Phase B (%)	Flow (mL/min)
Atenolol	Waters	0.1% FA	0.1% FA in	0.00	100	0.0	0.6
Antipyrine	VanGuard BEH	in MilliQ	ACN	1.11	100	0.0	
	C-			6.00	90	10	
	18 (2.1x 5 mm;			8.00	74	26	
	1.7 µm			9.00	0.0	100	
				10.00	0.0	100	
	Water Acquity-			10.10	100	0	
	BEH C-18 (2.1x			12.00	100	0	
	100mm; 1.7)						

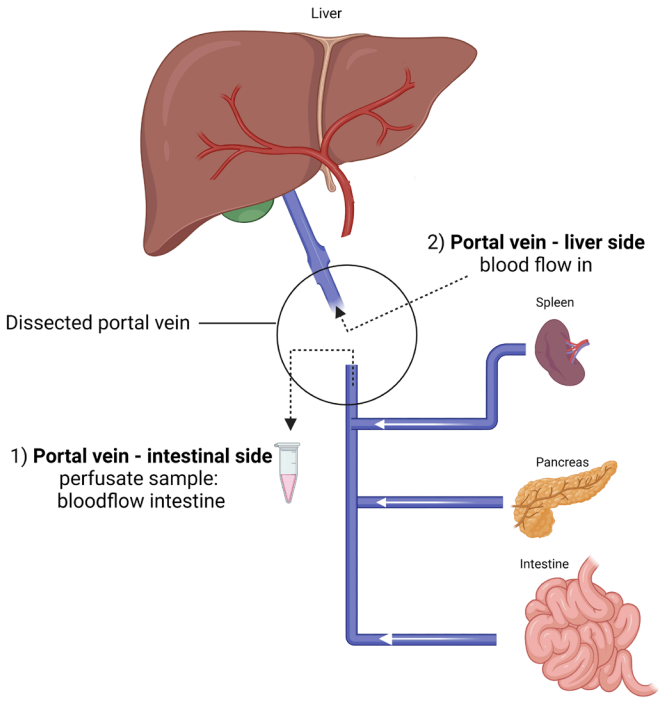

Figure S6.1 - Schematic representation of the dissected portal vein. By dissecting the portal vein, cannulation of the portal vein to the intestinal side is visualized allowing for collection of the portal venous outflow. The portal vein – liver side is also cannulated for an additional flush of the liver during the isolation procedure and to apply a portal flow during NMP.

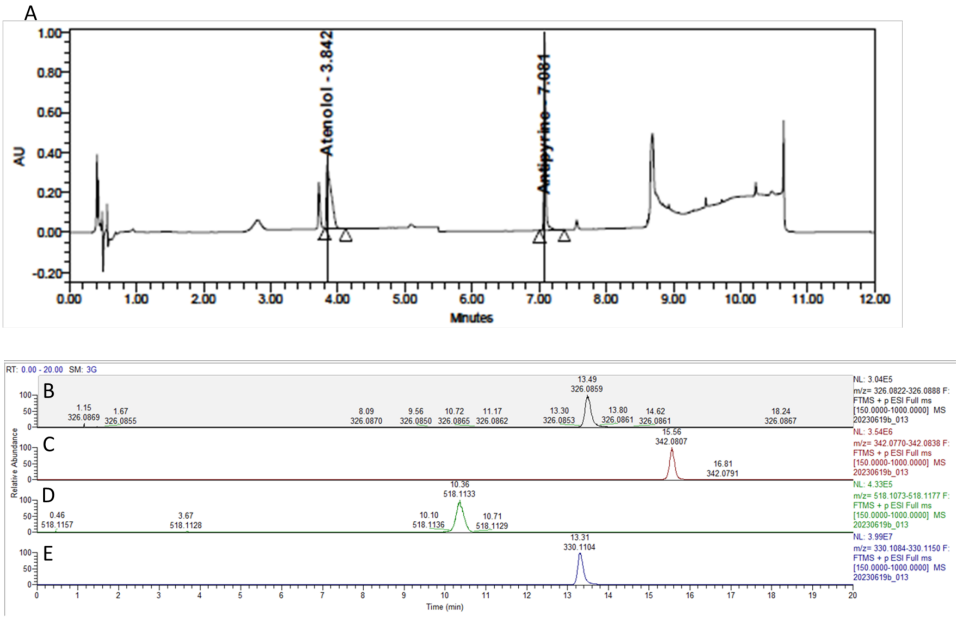

Figure S6.2 - Chromatograms of antipyrine, atenolol, midazolam and midazolam metabolites. (A) Detection of atenolol and antipyrine, (B) midazolam, (C) midazolam 1-OH, (D) midazolam 1-OH glucuronide and (D) midazolam internal standard.

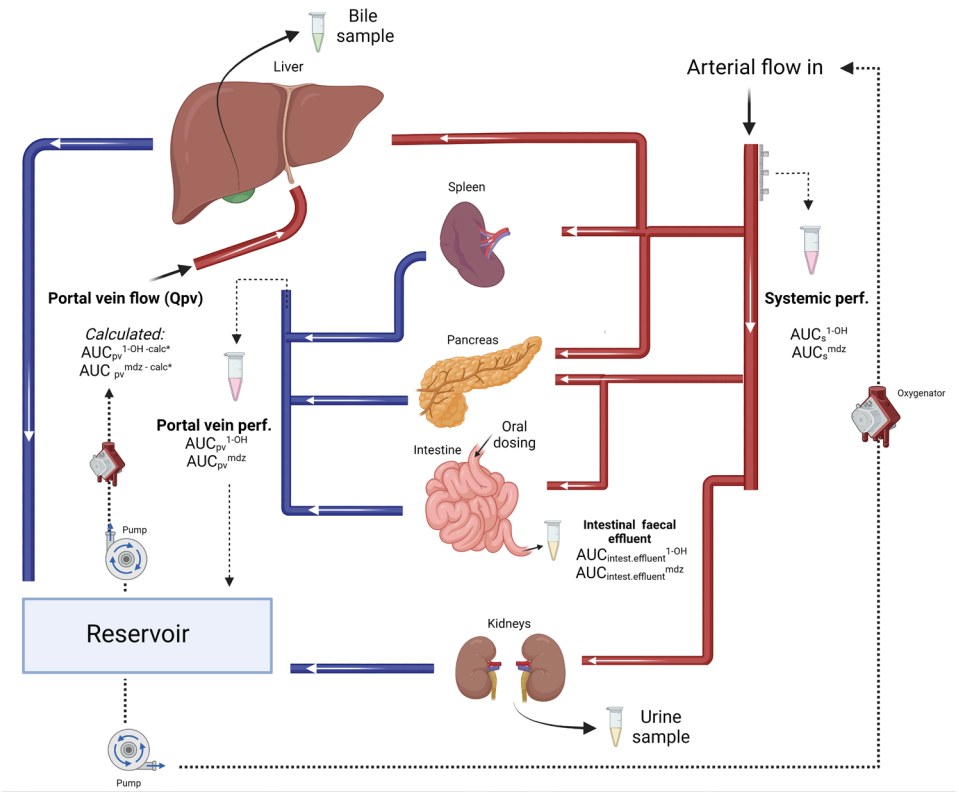

Figure S6.*3* - Schematic representation of concentration measurements of midazolam and metabolites.

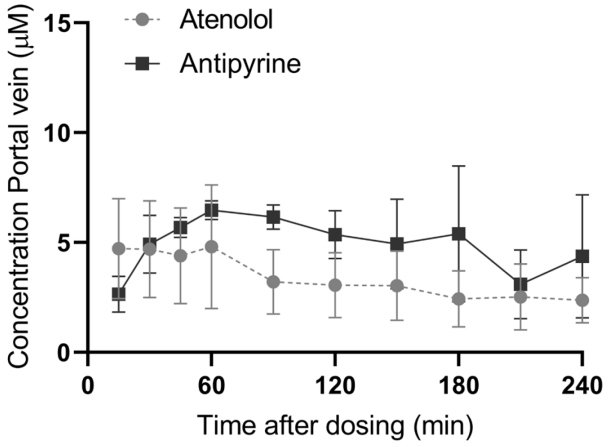

Figure S6.4 - Concentration of Atenolol (µM) and Antipyrine (µM) measured in the portal vein. Data shows average concentration of n=4 experiments ± SEM

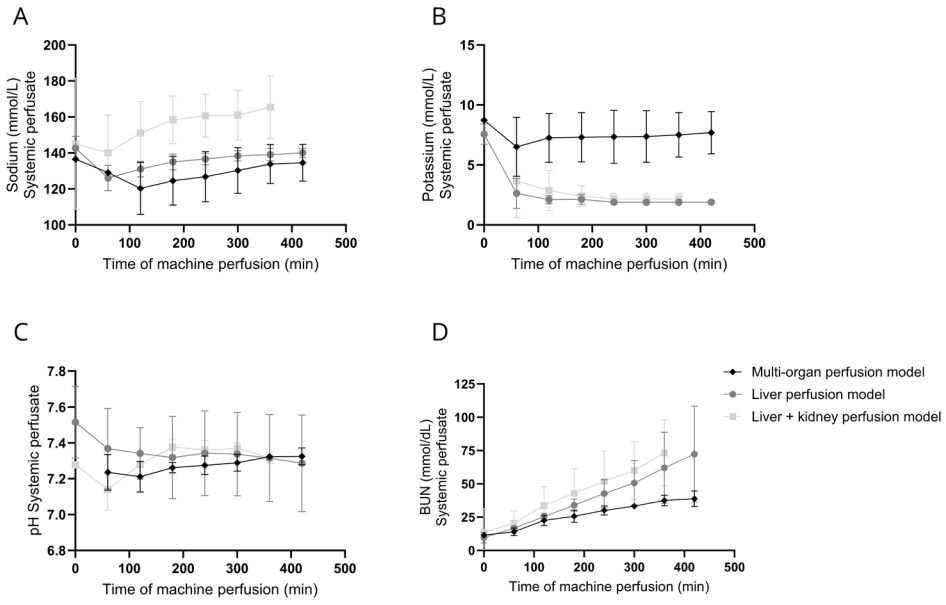

Figure S6.5 - Comparison of systemic perfusate levels of sodium, potassium, pH and BUN between multi-organ perfusion model, liver only and liver+kidney combined perfusion. (A) sodium levels in the systemic perfusate are relatively lower throughout the perfusion compared to liver only and combined liver+kidney perfusion. (B) Potassium levels in the systemic perfusate remain constant and measurable. Both the liver and combined liver+kidney perfusion model show a rapid decline in potassium levels which are <2 after 180 min of perfusion. (C) pH levels in systemic perfusate remain constant throughout the perfusion without the need for bicarbonate supply. (D) Blood urea nitrogen (BUN) levels measured in the systemic perfusate increase in all conditions however remain the lowest in the multi-organ model compared to the liver only and combined liver+kidney perfusion model.

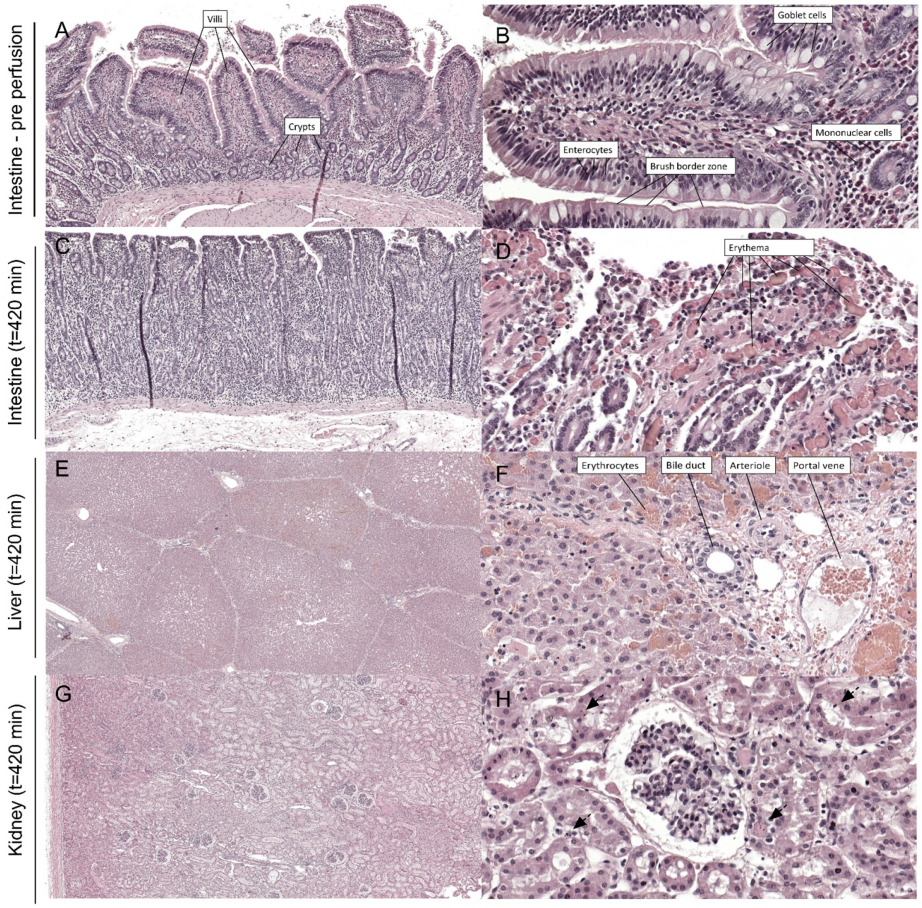

Figure S6.6 - Histological overview of intestine, liver and kidney. (A) H&E staining of the small intestine, taken after flush and before the start of the perfusion of the excised small intestinal tissue, showed intact palisade enterocytes at the villi (40x), (B) visibility of the enterocytes and goblet cells (200x). (C) After 420 min of perfusion partly intact epithelial layer of the intestine was observed, including presence of the villi with enterocytes and goblet visible (40x). (D) In 3 out of 4 studies vessel dilation (erythema) was observed (200x). (E) Morphology of the liver; chord structure was maintained with minimal to mild multifocal hepatocellular single cell necrosis associated with dilated sinusoids (E) Presence of erythrocytes in the portal venous area (200x) (G) Morphology of the kidney; Intact glomeruli were detected in all kidney slices (40x) (G) mild to moderate tubular single cell necrosis was present as indicated by the arrows (200x).

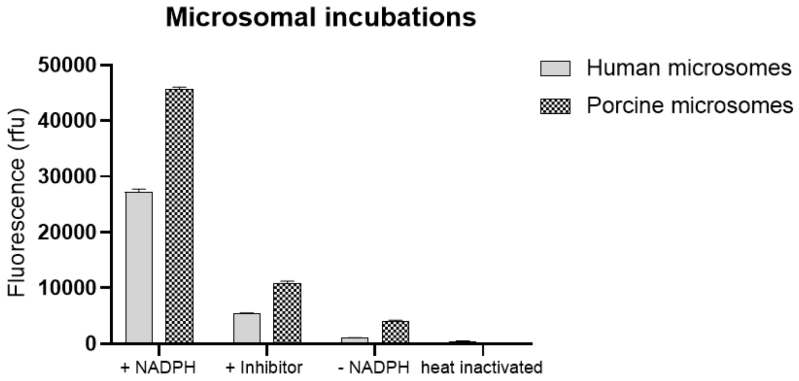

Figure S6.7 - CYP3A4 activity assessment in human and porcine microsomal fractions. CYP3A4 activity was measured using the VIVID red CYP3a4 activity kit with different conditions. To study CYP3A4 activity microsomes were incubated +NADPH. As control conditions, CYP3a4 activity in combination with: + 10 µM inhibitor (ketoconazole), -NADPH and heat inactivated microsomes was determined. Data shows mean ± SD n=3 (one individual experiment).

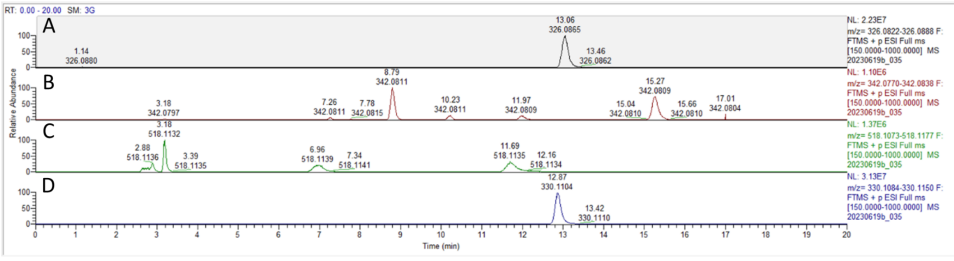

Figure S6.8 - Chromatogram of portal vein sample, 120 min after intraduodenal dose of midazolam (20 mg) showing multiple midazolam metabolites. (A) midazolam, (B) 1-OH midazolam, (C), 1-OH midazolam glucuronide and (D) midazolam internal standard.